Proceedings of the 11th International IEEE Conference on Intelligent Transportation Systems Beijing, China, October 12-15, 2008

Evaluation of Road Marking Feature Extraction

Thomas Veit, Jean-Philippe Tarel, Philippe Nicolle and Pierre Charbonnier

***Abstract*— This paper proposes a systematic approach to evaluate algorithms for extracting road marking features from images. This specific topic is seldom addressed in the literature while many road marking detection algorithms have been proposed. Most of them can be decomposed into three steps: extracting road marking features, estimating a geometrical marking model, tracking the parameters of the geometrical model along an image sequence. The present work focuses on the first step, i.e. feature extraction. A reference database containing over 100 images of natural road scenes was built with corresponding manually labeled ground truth images (available at `http://www.lcpc.fr/en/produits/ride/`). This database enables to evaluate and compare extractors in a systematic way. Different road marking feature extraction algorithm representing different classes of techniques are evaluated: thresholding, gradient analysis, and convolution. As a result of this analysis, recommendations are given on which extractor to choose according to a specific application.**

I. Introduction

The extraction of road markings is an essential step for several vision-based systems in intelligent transportation applications as for example Advanced Driver Assistance Systems (ADAS). Of course, these applications include lane detection for the lateral positioning of vehicles. But, maintenance tasks such as road marking quality assessment and more generally road scene analysis also rely on a precise computation of the position of road markings.

Most road marking detection algorithms consist of the following three steps:

1) road marking feature extraction,
2) geometrical model estimation,
3) tracking and filtering of the parameters of the geometrical model along an image sequence.

This article focuses on the first step when applied on all the image. The main reason for this is that a performance improvement at this stage will be beneficial to the following steps of the process. Another reason is that, depending on the application, the second and third step do not always exist, while the first is present in all applications based on road marking analysis, even in expectation based approaches (specifically, in the re-initialization process).

Different extractors have been proposed over the years to estimate the position of road markings parts in images. These extractors are based on the characteristics of the road markings, either geometric, photometric or both. The aim of the present work is to assess the performance of these extractors on a reference database and to issue some recommendations on which extractor suits for which application. This evaluation does not only rely on the performance of the extractors in terms of detection. It also points out other characteristics of the algorithms such as their computational complexity or the need for additional knowledge to achieve a given performance level.

The paper is structured as follows. Section II presents related work. Section III describes the six road marking extraction algorithms and the two variants which are evaluated. The database built for the evaluation, the ground truth labeling process and the evaluation metrics are detailed in Section IV. Section V discusses the experimental results obtained after processing the reference database with the six algorithms. Finally, Section VI gives concluding remarks and perspectives.

II. Related work

Despite the fact that road feature extraction is the first step of any lane detection system, it is too often partially described in papers describing marking detection, even if numerous variants were proposed. A thorough survey of lane detection systems is proposed in [1]. For a broader study of video processing applied to traffic applications (including lane detection) the reader is also referred to [2]. In this paper, six representative road feature extractors and two variants based on thresholding, gradient analysis and convolution were selected. For the subsequent steps involved in lane marking detection systems, the reader is referred to [3] for a robust version of the estimation step and to [4] for the tracking step.

To our knowledge, only a small number of papers about road marking detection include systematical evaluation results. Moreover, detection systems are most of the time evaluated *as a whole*. For example, in [1] a GPS based ground truth is built using a second downward looking camera and the evaluation metrics are only related to the lateral position of the vehicle. A lane detection system is also evaluated on synthetic images in [5]. Again, the whole lane detection system is evaluated by analyzing

T. Veit is with LIVIC (INRETS/LCPC), 14 route de la Minière, F-78000 Versailles France, `Thomas.Veit@inrets.fr`

J.-P. Tarel is with LCPC, 58 Bd Lefebvre, F-75015 Paris, France, `Jean-Philippe.Tarel@lcpc.fr`

P. Nicolle is with LCPC Nantes, Route de Bouaye, BP 4129, F-44341 Bouguenais, France, `Philippe.Nicolle@lcpc.fr`

P. Charbonnier is with LRPC Strasbourg (ERA 27 LCPC), 11 Rue Jean Mentelin, BP 9, F-67200 Strasbourg, France, `Pierre.Charbonnier@developpement-durable.gouv.fr`

the error on the estimated parameters of the geometrical road model.

A systematical evaluation of the extraction step, as we propose in this paper, involves associating a ground truth to every image of the test set. This can be fastidious when large image sets are considered. Automatic ground truth determination has been proposed in [6] based on thresholding. The main advantage of this technique is to allow automatically labeling large image sets, even it is still error prone and needs to be supervised. We thus preferred to label ground truth images manually in order to obtain higher accuracy. Let us note that the evaluation framework proposed in [6] was applied to small windows around road markings and not the whole road scene image.

III. Road markings extraction algorithms

Many local extraction algorithms for road marking features have been proposed. We restrict ourselves to algorithms extracting features from a single image captured by a camera in front of a vehicle. Extractors based on motion or stereo will not be considered. Markings are standardized road objects. More specifically, lane markings are bands of a particular width painted on the roadway, most of the time in white. Hence, single image extractors are generally based on two kinds of characteristics: geometric and photometric. These criteria are generally combined in different ways, and used often partially, depending on the local extraction algorithm. Existing road feature extractors can be classified with respect to the kind of feature they rely on:

- geometric selection: segments [7],
- geometric and photometric selection: pair of positive and negative gradients [8], [9], [10], [11], response to a convolution filter at a given scale [12], [1], ridges at a given scale [5],
- photometric selection: light pixels [13], [14], [15], edges [4], [16].

The set of extractors we compare in this paper ranges from mainly geometric selection to mainly photometric selection. They will be presented in this particular order. In all that follows, T_G will denote the detection threshold. This threshold is either on the intensity level, the magnitude of the gradient or a filter response in gray levels. Different kinds of (possibly partly worn out) markings may be present in an image. Therefore, it is reasonable to define an acceptability range, $[S_m, S_M]$, for selecting horizontal segments as road marking elements, depending on their width in pixels.

Our comparison is not exhaustive, and other marking feature extraction algorithms, such as morphological based, texture based or learning based extractors, which are seldom discussed in the literature, will not be taken into consideration. We also mainly focus on lane markings rather than special markings such as arrows or crossings.

A. Positive-negative gradients

The positive-negative gradients extractor is mainly based on a geometric selection with respect to feature width, see [8], [9], [10], [11]. Due to the perspective effect, this width constraint can be handled in two possible ways. Both approaches rely on a planar road assumption and the knowledge of the horizon line.

The first approach consists in performing an *inverse perspective mapping*, to build a top-view image of the road [9]. The second one consists in taking into account that the marking width decreases linearly in the image from the bottom to the horizon line and reaches zero at the horizon line [8], [10], [11]. This implies that the minimal width $S_m(x)$ and the maximal width $S_M(x)$ are linear functions of the vertical image coordinate x. The second approach is in practice faster and will thus be used in the positive-negative gradient algorithm.

This algorithm processes each image line below the horizon independently, in a sequential fashion. It first selects positive intensity gradients with a norm greater than a given threshold, T_G. Then, the algorithm looks for a pair of positive and negative gradients fulfilling the width constraint. For each image line x, let y_{init} be a horizontal image position for which the horizontal gradient is greater than the threshold T_G. Let y_{end} be the pixel position where the horizontal gradient is lower than $-T_G$. The sign of the threshold is selected in order to extract dark-bright-dark transitions. A marking feature is extracted if $y_{end} - y_{init}$ lies within the range $[S_m(x), S_M(x)]$ and if the image intensity between y_{end} and y_{init} is higher than the image intensity at y_{end} and y_{init}. The extracted feature is the segment $[y_{init}, y_{end}]$.

Contrasts being smooth in general, the positive-negative gradient algorithm may detect several beginning position y_{init} associated to the same marking. To tackle this problem, the extractions are superimposed in an extraction map, of the same size as the image. We also experiment with another variant where only local intensity gradient maxima greater than T_G are selected as in [9], rather than using all gradients higher than T_G. This local maxima variant is tested in our experiments under the name "strong gradient".

Notice that this extractor is specifically designed for markings that appear vertical in the image, so horizontal markings in the image will not be selected. However, due to the width tolerance this extractor is also able to detect curved markings.

B. Steerable filters

In the positive-negative gradient algorithm, each line is processed independently, the spatial continuity of lane markings is not exploited. This can be a handicap when deeply eroded markings are present. Steerable filters were applied for marking extraction in [1]. This kind of filter, able to extract bright stripes, is appealing since it allows to perform image smoothing and to select markings both with geometric and photometric criteria. Sharing some

similarities with steerable filters is the ridge detector proposed in [5].

The main advantage of steerable filters is that they are obtained as linear combinations of three basis filters corresponding to the second derivatives of a two-dimensional Gaussian distribution:

- $G_{xx}(x,y) = -\frac{1}{\sigma^2}\left(\frac{x^2}{\sigma^2}-1\right)\exp\left(-\frac{x^2+y^2}{2\sigma^2}\right)$,
- $G_{yy}(x,y) = -\frac{1}{\sigma^2}\left(\frac{y^2}{\sigma^2}-1\right)\exp\left(-\frac{x^2+y^2}{2\sigma^2}\right)$,
- $G_{xy}(x,y) = \frac{xy}{\sigma^4}\exp\left(-\frac{x^2+y^2}{2\sigma^2}\right)$.

The linearity of convolution enables to compute the response to the filter $G_\theta = G_{xx}\cos^2\theta + G_{xy}2\cos\theta\sin\theta + G_{yy}\sin^2\theta$ for any orientation $\theta \in [-\frac{\pi}{2}, \frac{\pi}{2}]$ as the following linear combination:

$$I_\theta = I_{xx}\cos^2\theta + I_{yy}\sin^2\theta + I_{xy}2\cos\theta\sin\theta, \qquad (1)$$

where I_{xx}, I_{yy} and I_{xy} stand for the intensity image convolved respectively with the basis filters G_{xx}, G_{yy} and G_{xy}.

Differentiating (1) with respect to θ yields the orientation, up to π, that maximizes the response of the steerable filter:

$$\theta_{\max} = \begin{cases} \frac{1}{2}\arctan\frac{I_{xy}}{I_{xx}-I_{yy}} & \text{if } I_{xx}-I_{yy} > 0, \\ \frac{1}{2}\left(\pi + \arctan\frac{I_{xy}}{I_{xx}-I_{yy}}\right) & \text{if } I_{xx}-I_{yy} < 0, \\ \frac{\pi}{4} & \text{if } I_{xx}-I_{yy} = 0. \end{cases} \qquad (2)$$

Let us note that these equations are the corrected version of those given in [1]. The orientation of the feature is constrained to the range $[-80°, 80°]$, where the origin of orientations corresponds to the vertical image coordinate axes, in order to reject horizontal ridges.

The variance parameter σ controls the scale of the filter, and one can show that the filter response is maximal for a perfect stripe of width 2σ. Therefore, σ is set to half the width of the markings to be detected in the image. Steerable filters can be applied optimally only to markings having one specific width. As a consequence, it is necessary to compensate the effect of perspective by a preliminary application of the inverse perspective mapping.

In order to evaluate the contribution of steerable filters to lane markings extraction, the vertical filter G_{xx} alone was also applied as a variant. This simplified filtering reduces the number of image convolutions from three to one and also avoids the computations of θ_{max} and the corresponding filter response.

In both cases, the final decision is given by a threshold T_G on the filter response.

C. Top-hat filter

Steerable filters are optimal for one marking width and are not able to tackle a large width range. We thus propose a top-hat filter which performs a convolution with a shape as shown in Fig. 1 similarly to [12], [8] but it is performed at many scales. Each line is processed independently, which avoids performing an inverse perspective mapping. Unlike steerable filters, the top-hat filter is dedicated to vertical lane markings.

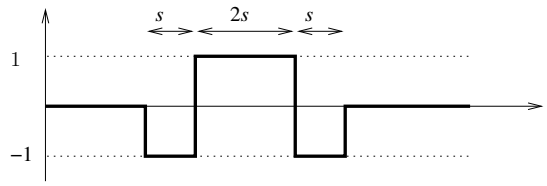

Fig. 1. *Top-hat filter for marking extraction.*

It is well known that the convolution with a top-hat filter can be performed in only 4 operations: $\frac{1}{4s}(2(C(y+s)-C(y-s))-(C(y+2s)-C(y-2s)))$, independently of its width $w = 4s$, by using the cumulative function of the intensity profile along each line, $C(y)$. This convolution is performed for several widths w and the local maxima in the feature space (w,y) are considered as marking features. The center of the marking element is given by the value of y at the maximum and its width, by w at the maximum. The final decision is made according to a threshold T_G on the filter response.

D. Global threshold

Markings being light on a gray background, a simple minded approach is to extract them locally by a global gray level thresholding with threshold T_G. It seems clear that this approach will not perform well due to variations of lighting conditions within the image [17]. However, we also included this purely photometric algorithm as a reference, to quantify the gain the other algorithms are able to achieve.

E. Local threshold

One way of tackling the problem of non uniform lighting conditions in a thresholding algorithm is to use local statistics of the image intensity within a small neighborhood of the current pixel. If (x,y) is the current pixel position, and $\bar{I}$ the local image intensity mean, the acceptance test is now $I(x,y) > T_G + \bar{I}(x,y)$. To deal with perspective, the averaging is performed independently on each line, and the size of the image averaging decreases linearly with respect to the line height. In practice, we set the averaging size to $12S_M(x)$. All extracted pixels are saved in an extraction map and horizontally connected features wider than $S_m(x)$ are selected as marking elements. This extractor mainly performs a photometric selection, followed by a partial geometrical selection.

F. Symmetrical local threshold

We experiment with another extractor which is mainly photometric, the so-called symmetrical local threshold. This extractor is a variant of the extractor first introduced in [13], [14]. Again, every image line is processed independently in a sequential fashion. On each line at position x, it consists of three steps. First, for each pixel at

position y, the left and right intensity averages are computed, i.e the image average $I_{left}(y)$ within $]y-6S_M(x),y]$ and the image average $I_{right}(y)$ within $]y,y+6S_M(x)]$. Second, given threshold T_G, the pixels with intensity higher than both T_G+I_{left} and T_G+I_{right} are selected. Third, sets of connected pixels in the extraction map wider than $S_m(x)$ are considered as marking elements.

G. Color images

The previously described algorithms implicitly assume that the input image is a gray level image. Colored elements of the scene may, however, appear as light gray in a luminance image. Hence, it is interesting to consider a colorimetric criterion in the decision process, as noticed in [8], [15]. To this end, our approach consists in first applying any of the previously described algorithms separately on each color channel and then, combining the three obtained extraction maps using a logical "and".

IV. Evaluation data set, ground truth labeling and evaluation metrics

A. Evaluation data set

To assess the performance of the marking feature extractors described in the previous section, we built a database of road scene images with ground truth.

The database contains 116 road scene images captured on various sites by the Network of the French Transportation Department. The images selection was performed with the objective of sampling:

- variable lighting conditions, such as shadows, bright sun, cloudy weather,
- variable scene content, from dense urban to countryside,
- variable road types, such as highway, main road, back-country road.

All the 116 ground truth images were manually labeled with three kinds of labels (see Fig. 2 for some examples):

1) lane markings, i.e. lateral road markings,
2) other kinds of road markings such as pedestrian crossings, highway exits lanes...
3) not a road marking.

To refine our analysis the database is also divided into three sub-classes:

1) curved road images,
2) adverse lighting conditions and eroded markings,
3) straight road under good lighting conditions and with good quality markings.

This database is available on LCPC's web site `http://www.lcpc.fr/en/produits/ride/` for research purpose and in particular to allow other researchers to rate their own algorithms. The proposed database is mainly designed for the evaluation of lateral road lane-markings extraction and will be completed and extended in the near future. However, we have anticipated over the development of this database by labeling also other kinds of markings in particular to allow the evaluation of more general road marking extractors.

B. Evaluation metrics

The comparison of the ground truth images with the extraction maps obtained by the different lane markings feature extractors presented in Sec. III enables to evaluate the performance of each extractor. All the presented extractors rely on a detection threshold T_G. Therefore, to evaluate the different algorithms objectively, the performances of each extractor is computed for all possible values of threshold T_G within the range $[0,255]$.

Two classical evaluation tools are used: Receiver Operating Characteristic (ROC) curves and Dice Similarity Coefficient (DSC, also named F-measure). ROC curves are obtained by plotting the True Positive Rate (TPR) versus the False Positive Rate (FPR) for different values of the extraction threshold T_G. The larger the area under the ROC curve, the better the extractor. Nevertheless, ROC curves should be analyzed carefully in case of crossing curves. Moreover, the proportion of pixels corresponding to lane markings in the image being small, about $1-2\%$, only the left part of the ROC curve is relevant for lane detection algorithms.

This is why we also use the DSC for complementary analysis. The DSC measures the overlap between the ground truth and the extraction maps provided by the different algorithms. It penalizes False Positives (FP) and is more suited for evaluating the detection of small image structures such as road markings. The Dice Similarity Coefficient is defined as:

$$DSC = \frac{2TP}{(TP+FP)+P} \tag{3}$$

where TP is the number of true positives, FP is the number of false positives and P is the number of positives to be detected. Plots of the DSC v.s. the value of T_G are shown in the next section. The value at the maximum of the DSC curve is of importance to compare the different extractors, since it corresponds in some way to an optimal value of the threshold T_G and the best possible performance of the algorithm. The width of the peak around the maximal value also informs on the sensitivity of the extractor with respect to the threshold tuning. The DSC is commonly applied in medical image analysis for evaluating the segmentation of small structures.

V. Experimental comparison

This section presents the results of the experimental comparison of the road marking extraction algorithms.

A. Results on the whole database

The six algorithms of Sec. III were applied to the whole images in the database. For each algorithm, the ROC and DSC curves are plotted on Fig. 3. ROC curves are plotted only in the range $[0\%,5\%]$ of False Positive Rate (FPR). Since the road markings represent about $1-2\%$ of the image, it makes no sense to analyze ROC curves when the FPR is above 5%. Furthermore, ratios $FP/(FP+TP)$ above 50% would imply robustness problems for

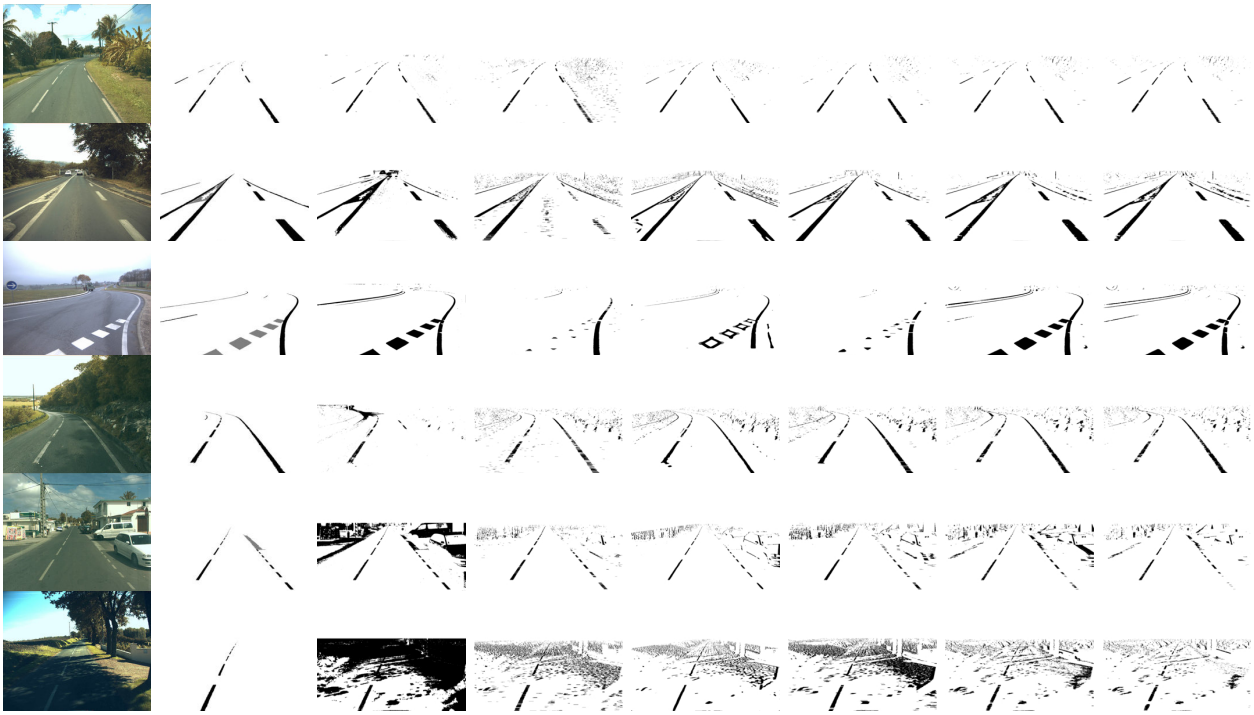

Fig. 2. First column original image. Second column ground truth (black: lane markings, gray: special markings, white: non-marking). Third-eighth column best extractions (in the sense of the Dice coefficient) with six different algorithms (from left to right): global threshold, +/− gradients, steerable filters, top-hat filter, local threshold and symmetrical local threshold.

the subsequent processing step, namely the geometrical model estimation. Most model estimation methods are unable to handle an *outlier* proportion larger than 50% in theory. The ROC curves are well suited for a broad ordering of method performance. For algorithm that have close performances, the DSC curves are more adapted.

From Fig. 3, we conclude that global thresholding is clearly not advisable even if the threshold is chosen optimally. However, the curves corresponding to the global threshold can be used as a reference to quantify the improvement obtained by the other extractors.

Positive-negative gradient performs slightly better than global thresholding but significantly worse than the four others. The four top extractors are, in decreasing order: symmetrical local thresholding, local thresholding, the top-hat filter and steerable filters. The fact that symmetrical local threshold performs best may be due to the simplicity of the assumed marking model. The variant of the positive-negative gradient extractor consisting in focusing on local maximum of the gradient performs even worse as shown on Fig. 4.

To our surprise, on the whole database steerable filters are outperformed. Their additional complexity is, hence, not justified. Moreover, the necessity of computing a perspective inversion of the image to obtain a constant width of the markings is clearly a drawback since it requires the knowledge of additional camera parameters. Invariance to orientation is not necessary and results in more false alarms. Results on the database are better when focusing on vertical ridges as shown on Fig. 5. The simpler variant consisting in applying only the vertical filter G_{xx} performs as well as the steerable filter, while it is computationally less expensive. The benefit of vertical averaging could not be established since the top-hat filter which is applied separately on each line performs as well as the steerable filters, if not better.

From our point of view, steerable filters are only justified if the geometrical model fitting step exploits orientation information. Indeed, steerable filters not only provide the position of the road marking features but also measure its orientation.

B. Results on subsets of the database

The first sub-database consists of images where the road marking are clearly visible and no specific difficulties prevent from detecting it. The performance of the top four extractors are closer to each other and the overall gain with respect to the simple global thresholding is reduced (cf. Fig. 6).

The second subset of images groups images that are especially difficult to process: low contrast of road markings, adverse lighting conditions (bright sun, shadows). This time the gap between the top four extractors and the simpler method becomes larger. Local thresholding extractors appear to be very well adapted for processing this type of images (cf. Fig. 7).

Finally, the last image subset consists of images with road markings presenting high curvature. As shown on

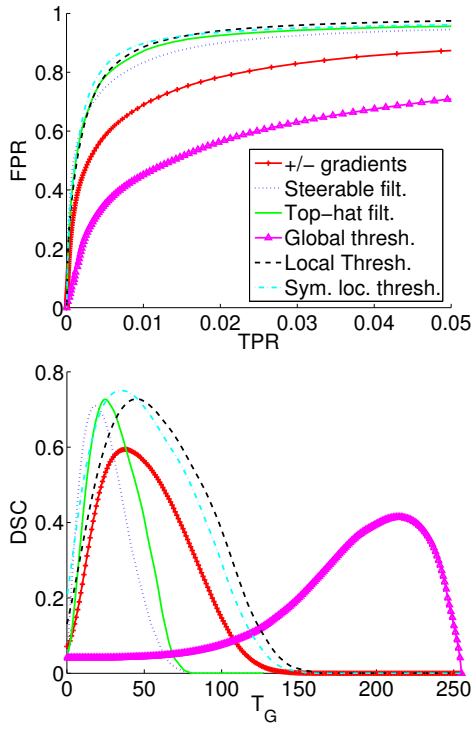

Fig. 3. ROC (top) and DSC (bottom) curves obtained for the 6 algorithms on the whole database.

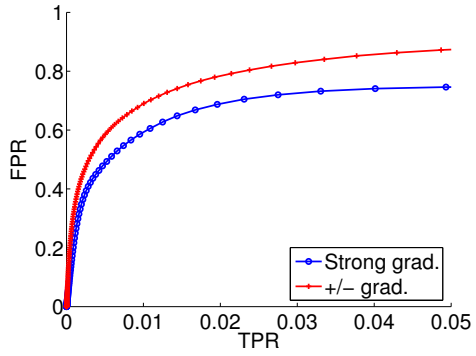

Fig. 4. ROC curves obtained on the whole database comparing +/−gradients and the variant with locally maximal gradients.

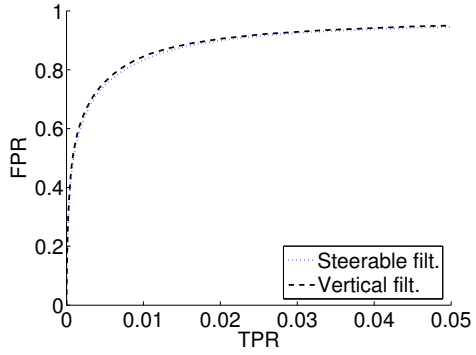

Fig. 5. ROC curves obtained on the whole database comparing steerable filter and vertical filter G_{xx}.

Fig. 8, on this subset the performance of the local thresholding extractors decrease. Let us emphasize that on this subset the vertical filter G_{xx}, the simpler variant of the steerable filters, still performs as well as the steerable filters themselves. On images presenting high curvatures of the road marking one could be surprised by the good performances of the extractors designed for detecting vertical marking only. This is explained by the tolerance of this extractors with respect to the width of the lane markings.

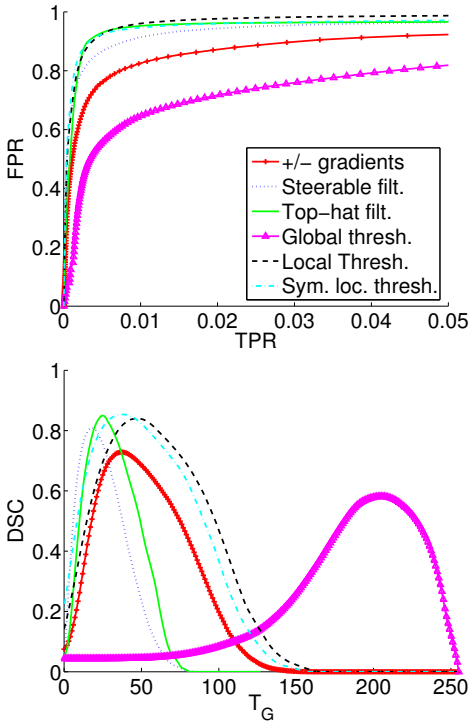

Fig. 6. ROC (top) and DSC (bottom) curves obtained on normal/easy images.

C. Taking color into account

We also evaluated the interest of using color images rather than gray level ones. Fig. 9 shows the ROC and dice curves obtained using symmetrical local threshold and positive-negative gradients extractors on gray level and color versions of the reference images. Looking at the left part of the ROC curve and at the maximal value of the dice curve, it is clear that the use of colors slightly improves results even if the extractor is more selective when using color images. The use of color, as explained in Sec. III-G should thus be advised. The width of the dice curves are roughly similar between gray levels and colors. In term of complexity, any extractor is three time slower on a color image than on its gray level version. Therefore, when maximum speed is a strong requirement, gray level images can be used with a slight loss in terms of performance.

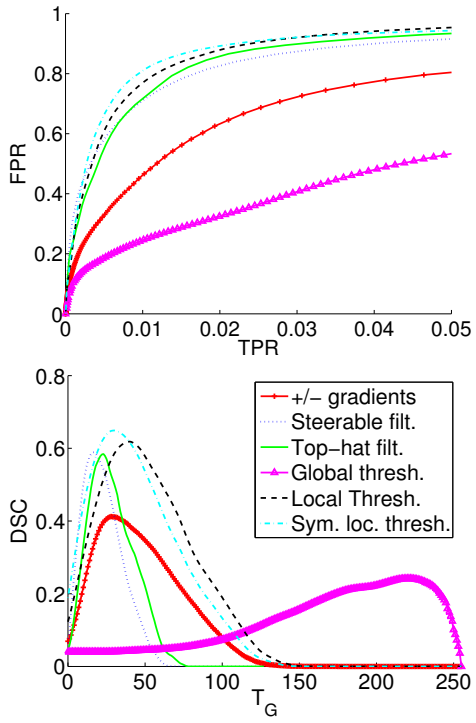

Fig. 7. ROC (top) and DSC (bottom) curves obtained for adverse lighting conditions.

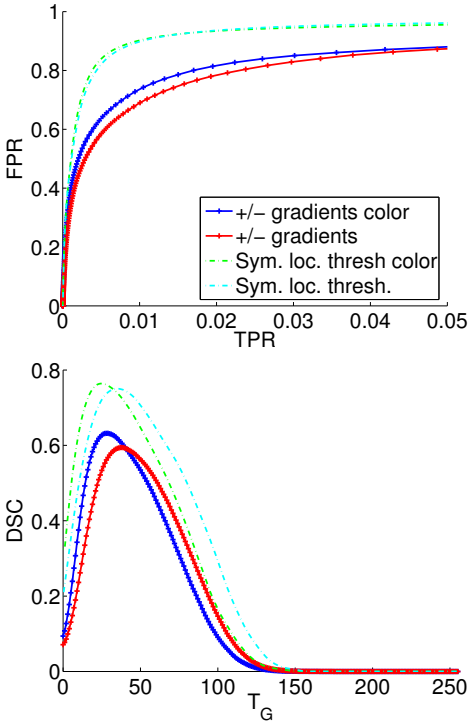

Fig. 9. ROC and dice curves obtained on the whole database without and with the use of image colors for symmetrical local threshold and positive-negative gradients extractors. The use of colors slightly improves results.

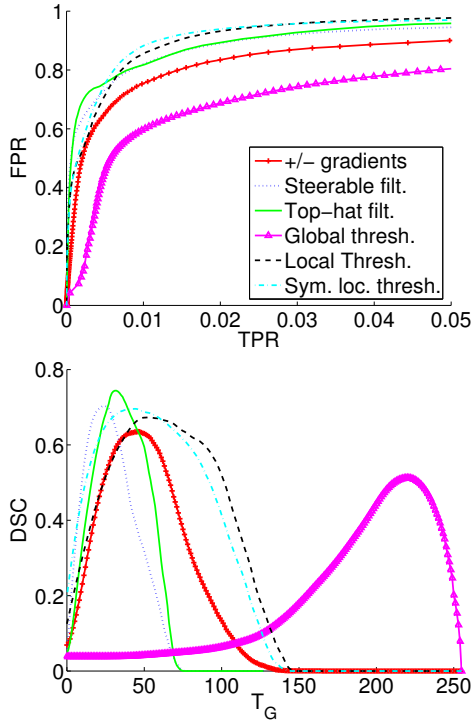

Fig. 8. ROC (top) and DSC (bottom) curves obtained for high curvature images.

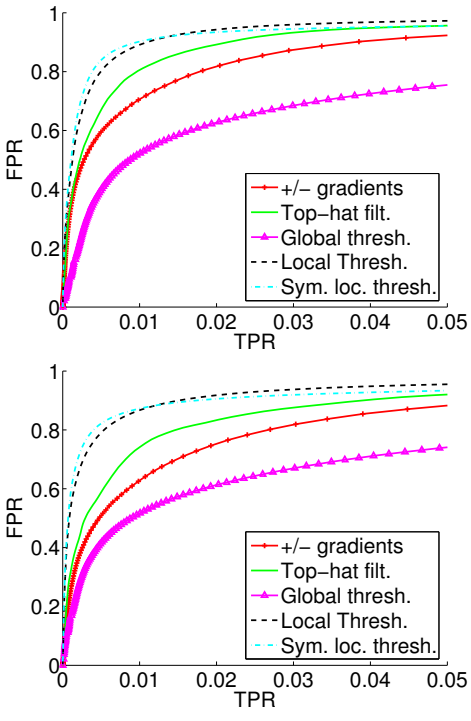

Fig. 10. ROC curves obtained with the five extractors with top, markings selected within $[5cm, 45cm]$ and lower within $[5cm, 90cm]$, for the whole database using color images.

D. Wide markings

Previous results were obtained for $[S_m, S_M] = [5cm, 20cm]$. In order to extract more general road markings such as zebras, arrows, pedestrian crossings, we experiment with the five extractors which are, by construction, suitable to extract marking within a given width range. Steerable filter are excluded since dedicated to a specific width. As shown in Fig. 3 for range $[S_m, S_M] = [5cm, 45cm]$ and Fig. 10 for range $[5cm, 45cm]$ and $[5cm, 90cm]$, the quality of the extraction slowly decreases when the range increases due to the increasing difficulty of the extraction task. It can be observed that the better performing extractors are not too sensitive to variations of input parameters such as the size range of marking extraction, which is an appealing property.

VI. Conclusion

We presented an experimental comparison study on six representative road feature extractors and two variants. These algorithms were selected to sample the state of the art in road marking detection. The comparison was performed on a database of 116 images featuring variable conditions and situations. A hand-made ground truth was used for assessing the performance of the algorithms.

Experiments show that photometric selection must be combined with geometric selection to extract road markings correctly. As usual in pattern recognition, this task is not trivial, even for objects that seem quite simple, such as road markings. In particular, pitfalls such as lousy models and too selective models must be avoided. The methodology we proposed in this paper is a helpful tool for this purpose. For example, several times during this study, we were faced with intuitively good variants, which appeared to be inefficient in practice when systematically evaluated on the test base.

As a result of our evaluation, it appears that for road marking extraction, the selection should be mainly based on photometric and colorimetric features, with just a minimal geometric selection. The extractor which gave the best result in the general case is the symmetrical local threshold. Nevertheless, it is not necessarily the optimal choice in particular cases such as curved roads, as observed in our experiments. Additive advantages of the symmetrical local threshold is its implementation simplicity and its reduced computational complexity compared to other extractors we experimented with, such as steerable filters. These conclusion must be also moderated by taking into consideration following next steps of detection process in particular when an expectation base approach is used.

Our goal is now to share our database with other interested researchers, in such a way that the number of compared extractors increases. We are also planing to extend the database to other scenarios (e.g. rain, night conditions, images taken behind a dirty windscreen) and to many other special road markings. The database can be also used in the future to evaluate the estimation and tracking steps independently and as a whole.

Acknowledgments

Thanks to LRPC Angers, Bordeaux, Nancy, Rouen and Strasbourg which provided us the road images. Some of these images are property of CG31, DDE88, DDE971, DDE974 and LCPC. Thanks also to the French Department of Transportation for funding, within the SARI-PREDIT project (http://www.sari.prd.fr/HomeEN.html).

References

[1] J. McCall and M. M. Trivedi, "Video based lane estimation and tracking for driver assistance: Survey, system, and evaluation," *IEEE Transactions on Intelligent Transportation Systems*, vol. 7, no. 1, pp. 20–37, March 2006.

[2] V. Kastrinaki, M. Zervakis, and K. Kalaitzakis, "A survey of video processing techniques for traffic applications," *Image and Vision Computing*, vol. 21, no. 4, pp. 359–381, April 2003.

[3] J.-P. Tarel, P. Charbonnier, and S.-S. Ieng, "Simultaneous robust fitting of multiple curves," in *Proceedings of International Conference on Computer Vision Theory and Applications (VISAPP'07)*, Barcelona, Spain, 2007, pp. 175–182.

[4] R. Chapuis, J. Laneurit, R. Aufrere, F. Chausse, and T. Chateau, "Accurate vision based road tracker," in *IEEE Intelligent Vehicles Symposium, IV'2002*, Versailles, 2002.

[5] A. Lopez, J. Serrat, C. Canero, and F. Lumbreras, "Robust lane lines detection and quantitative assessment," in *3rd Iberian Conference on Pattern Recognition and Image Analysis*, Girona, Spain, June 2007.

[6] K. Kluge, "Performance evaluation of vision-based lane sensing: somepreliminary tools, metrics, and results," in *IEEE Conference on Intelligent Transportation System*, 1997.

[7] F. Guichard and J.-P. Tarel, "Curve finder combining perceptual grouping and a Kalman like fitting," in *IEEE International Conference on Computer Vision (ICCV'99)*, Kerkyra, Greece, 1999.

[8] K. Kluge and C. Thorpe, "The YARF system for vision-based road following," *Mathematical and Computer Modelling*, vol. 22, no. 4-7, pp. 213–233, August 1995.

[9] A. Broggi and S. Bertè, "Vision-based road detection in automotive systems: a real-time expectation-driven approach," *Journal of Artificial Intelligence Research*, vol. 3, pp. 325–348, 1995.

[10] J. Goldbeck, B. Huertgen, S. Ernst, and F. Wilms, "Lane following combining vision and DGPS," *Image and Vision Computing*, vol. 18, no. 5, pp. 425–433, April 2000.

[11] S.-S. Ieng, J.-P. Tarel, and R. Labayrade, "On the design of a single lane-markings detector regardless the on-board camera's position," in *Proceedings of the IEEE Intelligent Vehicles Symposium*, 2003.

[12] D. Aubert, K. Kluge, and C. Thorpe, "Autonomous navigation of structured city roads," in *SPIE Mobile Robots*, 1990.

[13] F. Diebolt, "Road markings recognition," in *International Conference on Image Processing*, vol. 2, Lausanne, Switzerland, September 1996, pp. 669–672.

[14] P. Charbonnier, F. Diebolt, Y. Guillard, and F. Peyret, "Road markings recogition using image processing," in *IEEE Conference on Intelligent Transportation System (ITSC)*, 1997.

[15] H.-Y. Cheng, B.-S. Jeng, P.-T. Tseng, and K.-C. Fan, "Lane detection with moving vehicles in the traffic scenes," *IEEE Transactions on Intelligent Transportations Systems*, vol. 7, no. 4, pp. 571–582, december 2006.

[16] R. Wang, Y. Xu, Libin, and T. Zhao, "A vision-based road edge detection algorithm," in *Proceedins of the Intelligent Vehicle Symposium*, Versailles, 2002.

[17] M. P. N. Burrow, H. T. Evdorides, and M. S. Snaith, "Segmentation algorithms for road marking digital image analysis," *Proceedings of the Institution of Civil Engineers. Transport*, vol. 156, pp. 17–28, February 2003.